On-chip AC Electrophoresis in Supported Lipid Bilayer Membranes.

ARTICLE *in* ANALYTICAL CHEMISTRY · NOVEMBER 2012

Impact Factor: 5.64 · DOI: 10.1021/ac302446w · Source: PubMed

6 AUTHORS, INCLUDING:

Peng Bao
University of Leeds
67 PUBLICATIONS **758** CITATIONS
SEE PROFILE

Johannnes S Roth
University of Leeds
5 PUBLICATIONS **12** CITATIONS
SEE PROFILE

Stephen D Evans
University of Leeds
227 PUBLICATIONS **6,268** CITATIONS
SEE PROFILE

analytical chemistry

Article

pubs.acs.org/ac

On-Chip Alternating Current Electrophoresis in Supported Lipid Bilayer Membranes

Peng Bao,[§] Matthew R. Cheetham,[§] Johannes S. Roth, Anita C. Blakeston, Richard J. Bushby, and Stephen D. Evans*

School of Physics and Astronomy, University of Leeds, Woodhouse Lane, Leeds LS2 9JT, United Kingdom

Supporting Information

ABSTRACT: By forming lipid bilayers within SU8 patterns, between interdigitated electrodes, we have demonstrated that it is possible to manipulate charged membrane components using low applied voltages over relatively short time scales. Two distinct patterns were studied: a nested "fish trap" which served as a molecular trap, and a diffusion aided Brownian ratchet which operated as a molecular pump. By reducing the size of the structures we have demonstrated that large applied fields (>200 V/cm) can be achieved on-chip, using low applied potentials (<13 V). By using ac fields applied orthogonal to the direction of desired motion, the molecular pumps provide a voltage independent method for moving charged components within lipid membranes over large distances. The reduced scale of the trap structures compared to those previously used in our laboratory has led to over a 10-fold decrease in the operational time require for charge build-up, from 16 h down to 1.5 h. The observed benefits of scaling means that these systems should be suitable for the on-chip separation and manipulation of charged species within supported lipid membranes.

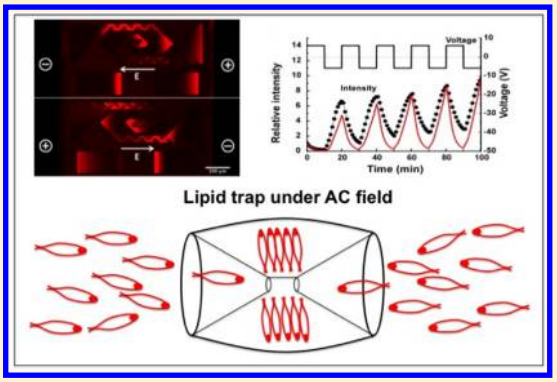

Lipid membranes play an essential role in cell function: controlling the exchange of nutrients and metabolites with their exterior environment, permitting the creation and sustainability of chemical and electrical gradients, and acting as a host for membrane proteins with a wide variety of functions. In recent years, supported lipid bilayers (SLBs) have been used as a biomimic of such cell membranes for studying fundamental biophysical/biochemical processes,[1−5] for applications in biosensing and diagnostics,[6−8] and as a platform for studying more complex processes, such as bacterial cell wall formation[9] or the light harvesting system.[10] Notwithstanding the importance of membrane proteins as targets for new drugs, and controlling cell function, the structures have only been solved for a small proportion of the many thousands coded for in the human genome. In large part this stems from the difficulty in manipulating them outside of their membranous environment, without loss of structure. Thus, new methods for the manipulation of such proteins within their membranous environment would be extremely important, and several methods are currently being explored, including hydrodynamic drag to manipulate protruding membrane components,[11−13] reduction in interfacial area in droplet interface bilayers,[14] or electric fields to reorganize charged membrane components.[15−22] Poo and Robinson first demonstrated that an external electric field applied across embryonic muscle cell membranes led to the movement of the membrane protein concanavalin A from one side of the cell to the other.[15,16] This idea was translated for use in supported lipid bilayers by Stelzle et al.,[19] and subsequently by the Boxer group.[20,21] Using a dc electric field applied tangentially to the surface of SLBs, charged lipids or proteins have been confined into narrow regions near patterned barriers.[19−22] Additionally, the effects of electrophoresis and electro-osmosis have been combined to separate proteins or charged lipids with different size/charge ratios in supported lipid bilayers into narrow bands under a steady electric field.[23] Some nanostructures have also been employed in combination with electric fields, which serve to rectify the random thermal movement of molecules. This was achieved through the use of nanosized Brownian ratchet structures in SLBs, such that components could be separated according to their diffusion coefficient.[24,25] Kashimura et al. have recently reported that electric fields could be used to control lipid spreading and therefore bilayer formation.[26] However, the methods mentioned above all used a dc electric field as the driving force, which implies that a high voltage is needed if the working distance is long.

Recently, we have demonstrated that charged lipids and a "simple" transmembrane protein can be concentrated in SLBs by using a "fish-trap" structure in conjunction with an ac electric field.[27] We have also shown the directed transport and orientational sorting of transmembrane proteins by using double-sawtooth ratchet patterns.[28] However, our previous work has two major shortcomings. First, large applied potentials (~200 V) were required to achieve suitable electric

Received: August 24, 2012
Accepted: November 9, 2012
Published: November 9, 2012

field strengths (~60 V/cm), and second, the time taken for any considerable build-up to be achieved was long (>10 h). These limitations were mainly due to the use of external electrodes (the gap between those electrodes was ~3 cm). In this paper, we have scaled-down the size of these ratchet patterns and incorporated them within interdigitated electrode systems making them more suitable for integration into on-chip systems. Consequently, the operating voltage was reduced by more than an order of magnitude (from 200 V down to 13 V or less), and the achievable electric field strength also rose by a similar factor. Importantly, we demonstrate that this miniaturization leads to a significant reduction in the operation time from around 16 h down to ~1.5 h. Further development is expected to inspire the production of nanoscale devices, with the appearance of portable lab-on-chip devices driven by batteries, which can separate and analyze lipid membrane samples on minute time-scales.

EXPERIMENTAL SECTION

Substrate Preparation. Glass coverslips of 22 mm × 26 mm × 0.1 mm (VWR Ltd., U.K.) were cleaned in acetone, isopropanol, and water for 5 min in an ultrasonicator, followed by piranha cleaning for 10 min at 80 °C. The glass plates were rinsed in deionized water thoroughly and then dried under a stream of nitrogen. They were then baked at 150 °C for 1 min to remove the moisture on the surface. S1805/PMMA double layers were used for the fabrication of Au/Ti interdigitated electrodes by the sputtering and lift-off method. The PMMA495K A3 (MicroChem. Corp.) was spin-coated onto the glass substrate at 4000 rpm for 30 s, before being baked on a hot plate for 10 min at 180 °C. After it was cooled down to room temperature, a second layer of S1805 photoresist was spin-coated at 5000 rpm for 30 s. The sample was then baked at 115 °C for 1 min. S1805 resist was patterned using standard photolithography methods. The S1805 pattern was transferred into the PMMA layer by exposing the sample with deep UV light, and subsequently soaking in PMMA developer. The resulting sample was cleaned by O_2 plasma etching at 50 W for 30 s before the Au and Ti metal layers were deposited at 100 and 10 nm, respectively, using a dc sputtering machine. The metal on the double layer resist was removed with acetone.

A thin layer of SU8 (~100 nm) (MicroChem. Corp.) was spin-coated onto the glass substrates that were prepatterned with Au/Ti interdigitated electrodes. The SU8 thin film was then patterned using normal photolithography methods with an exposure dose of 60 mJ/cm^2, following the procedure suggested by MicroChem.

Preparation of Lipids. For the preparation of lipids, 1 mg of L-α-phosphatidylcholine (EggPC) lipids (Avanti Polar Lipids Inc., Alabaster, AL) and 0.5 mol % Texas Red 1,2-dihexadecanoyl-sn-glycero-3-phospho-ethanolamine (TR-DHPE) (Invitrogen Ltd., Paisley, U.K.) were dissolved in a 50:50 mixture of chloroform/methanol. The mixture was then dried under a nitrogen flow for 1 h to remove all the solvent, and the dried lipid mixture was subsequently resuspended in 1 mL of phosphate buffered saline (PBS) solution. Small unilamellar vesicles (SUVs) were produced by 30 min tip-sonication, at 4 °C, using a Branson sonifier (Branson Ultrasonics Corp., Danbury, CT). The resulting suspension was centrifuged for 1 min at 14 500g in order to remove any residual titanium particles deposited by the tip. The supernatant was diluted with PBS to give a concentration of EggPC around 0.5 mg/mL. It was then used as fresh or kept in a refrigerator at 4 °C for up to a few days.

Formation of Lipid Bilayers. The glass substrates with SU8 patterns were cleaned in a UV-ozone cleaner for 30 min. They were then incubated with the SUV suspension described above for 60 min at room temperature in a home-built flow cell. Supported lipid bilayers were formed on the hydrophilic surface of glass due to the spontaneous rupture of SUVs. No bilayer formation occurred in the regions with SU8 pattern. Excess SUVs in solution were then rinsed away with degassed Milli-Q water.

Fluorescence Microscopy. The fluorescence signal from fluorophores in the supported lipid bilayer was observed using an epifluorescence microscope (Nikon Instruments Europe B.V., Kingston, U.K.) equipped with a Texas Red filter block. Fluorescence images were captured using a 12-bit greyscale digital camera, Orca-ER (Hamamatsu Photonics UK Ltd., Welwyn Garden City, U.K.). Regarding postprocessing, the relative intensity was calculated as the ratio between the mean fluorescence intensity in the labeled reservoirs and that in the whole enclosed lipid bilayer pattern, after subtracting the background intensity from both. The mean fluorescence intensity in the entire pattern was used as the reference, in an attempt to eliminate the effects of photobleaching during image acquisition as well as to eliminate some of the effects of self-quenching (see later in the Results and Discussion section) of TR-DHPE when it was concentrated against the SU8 pattern by the electric field.

Electrophoresis. An arbitrary waveform generator (Thurlby Thandar Instruments Ltd., Huntingdon, U.K.) was used to generate the electrical signal used in the experiments. A home-built flow cell was used to keep the membrane in an aqueous environment and enable the connection of external electrodes with the on-substrate interdigitated electrodes. Currents of 10−100 μA between the electrodes were monitored using a Keithley Picoammeter (Keithley Instruments Ltd., Theale, U.K.). Oxidation and reduction at the two electrodes was necessary to prevent the build-up of an electric double-layer. A constant flow of degassed Milli-Q water at 0.75 mL/min was used throughout the experiment to reduce any Joule heating generated by the electric current, maintain a constant temperature, and also to dissolve away any gas bubbles generated in oxidation and reduction near the electrode surfaces. The movement of charged lipid was monitored by fluorescence microscopy as mentioned above.

Computer Modeling. Finite element analysis (FEA) software COMSOL Multiphysics was used to solve the partial differential equations that describe diffusion and electrophoretic migration in this system. Details of the exact model setup, including the boundary conditions and postprocessing, can be found in the Supporting Information.

RESULTS AND DISCUSSION

Charged Lipid Concentration in "Nested" Traps. A schematic diagram of the experimental setup is shown in Figure 1. A flow cell was used to maintain the aqueous environment for the lipid bilayer and to provide a constant water flow. The bilayer, consisting of 99.8 mol % EggPC lipid/0.2 mol % TR-DHPE, was formed on the prepatterned glass substrate using the vesicle fusion method,[18,19] and was visualized by epifluorescence microscopy.

Interdigitated Au/Ti electrodes and the patterned SU8 structures were photolithographically formed on the coverslip.

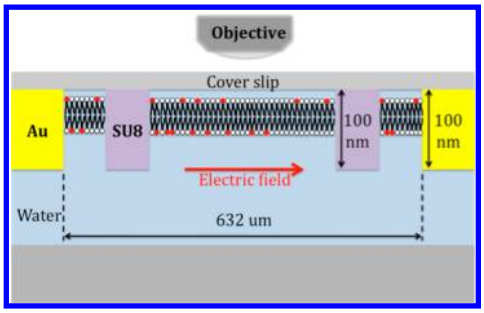

Figure 1. Schematic diagram showing the experimental setup. The EggPC lipid bilayer doped with TR-DHPE (0.2% mol) was formed on a glass coverslip, between the "fingers" of an interdigitated Au/Ti electrode array. An ac electric field was applied between these electrodes, inducing migration in the charged components of the SLB patches.

The SU8 was patterned to create smaller-scale versions of nested traps and membrane pumps as recently described by our group.[27,28] An ac square-wave signal of amplitude of 6 V (equivalent to an electric field strength, E, of ±95 V/cm for the pattern shown in Figure 2) and period of 20 min was applied in the plane of the lipid bilayer, in the direction indicated in the figure. The negatively charged TR-DHPE lipid migrated in phase with the ac field due to the electrophoretic force. Prior to the application of the electric field, the negatively charged TR-DHPE was uniformly distributed in the lipid bilayer pattern (Figure 2a). Once the field was applied, the TR-DHPE lipid moved toward the positively biased electrode (Figure 2b). The TR-DHPE in region 1 (see Figure 2a) moved toward region 6, where it was held against the SU8 barrier by the electric field. Simultaneously, TR-DHPE in region 2 moved into region 5, and was also held there due to the local shape of the pattern. Upon reversal of the field, the TR-DHPE began moving to the left (Figure 2c). This time, however, in addition to TR-DHPE in region 7 moving toward region 2, the TR-DHPE that had previously been trapped in regions 6 and 5 was moved to regions 3 and 4, respectively. The "teeth" along the edges of the outermost regions were included to prevent the back flow of material on field reversal. Such nested "traps" were designed to make it easy for the TR-DHPE to enter the next layer inward but difficult to move outward. Repeated cycling of the ac field thus caused a net build-up toward the center of the pattern. (See supplementary video in the Supporting Information for the movement of TR-DHPE in the lipid bilayer.)

Figure 3 shows the change in relative intensity of TR-DHPE in regions 3−5 as a function of time. The black circles represent the experimental data, and the red curves were obtained by finite element calculations. The relative intensity in regions 3 and 5 (Figure 2a) displayed a rapid 6-fold increase during the first cycle followed by a more gradual increase thereafter. This result shows the same general behavior as that of our previous experiments with larger traps, but now with an order of magnitude reduction in the operational voltage and the required time periods. The curves are not saturated after 5 cycles, and it is anticipated that higher concentrations could be realized by applying the field for more cycles. Further, it is possible to operate the system at lower voltages <5 V, using longer time periods, or at higher voltages to reduce the time period. As an example, an experiment was performed using an ac signal of amplitude 10 V, and a period of 5 min, which produced an 8-fold build-up in 30 min (see the Supporting Information).

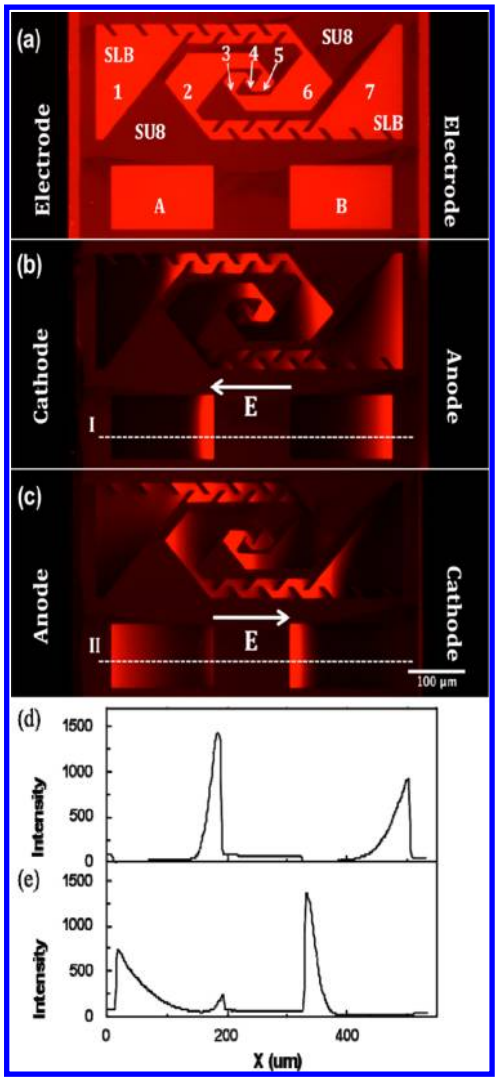

Figure 2. Fluorescence images showing the charged TR-DHPE (bright red region) in a nested trap pattern, under the influence of an ac square wave electric field. The lipid bilayer is formed on bare glass surrounded by an SU8 pattern (dark red region). (a) Before the application of an electric field. TR-DHPE is uniformly distributed in the bilayer. (b) After application of an electric field for 10 min (half a period). Negatively charged TR-DHPE migrated toward the anode, and was transferred from the large outer reservoirs to the smaller inner reservoirs. (c) After application of an electric field for 20 min (one full period). The TR-DHPE was built-up against barrier in the reversed direction. (d and e) Profiles of the fluorescence intensity taken along the dashed lines I and II, respectively (as shown in parts b and c), across the two rectangular reference patterns in the lipid bilayer.

Finite element analysis was used to model the behavior of the charged components of the SLB. The model was similar to that described previously, and further details on the exact model setup are described in the Supporting Information.[27,28] The red curves seen in Figure 3 are the result of the finite element calculations. To obtain good agreement between the simulation and experiment a reduced "effective mobility", μ^*, was introduced (eq 1)

$$\mu^* = \alpha\mu = \alpha D^*/k_B T \quad (1)$$

where the parameter α accounts for the reduction in the drift velocity due to electro-osmotic drag[19−21] and D^* is the effective diffusion coefficient. Previous work has reported an α value of

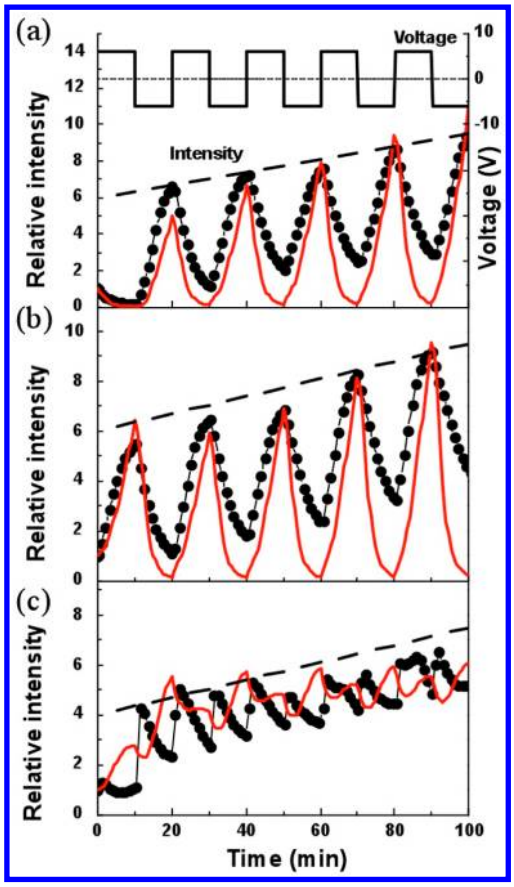

Figure 3. (a–c) Relative intensity of TR-DHPE in reservoirs 3, 5, and 4, respectively (as labeled in Figure 2a), as a function of time. Experimental results: black dotted lines. Finite element calculations: red curves. The relative intensity is calculated as the ratio of the mean fluorescence intensity in the reservoir regions and the mean fluorescence intensity in the whole lipid pattern, after subtracting the background intensity. The highest relative intensity in reservoir 3 and 5 is 9.7. The applied square wave signal can be seen at the top of the figure.

about 0.6 for TR-DHPE to describe the steady-state behavior.[19−21] The effective diffusion coefficient, which was reduced from the typical diffusion coefficient of 1.5 $\mu m^2/s$ that was found for TR-DHPE, also had to be used to obtain a good fit between FEA calculations and experiments. This additional reduction appears to be most significant in the smaller, more confined regions of the pattern, and may arise due to local changes in the lipid composition (increased TR-DHPE) leading to an increase in the phase transition temperature and hence a reduced diffusion coefficient. Alternatively, it is possible that TR-DHPE may form dimers when present at sufficiently high concentration. If this occurs, it is possible that the charge or diffusion coefficient of the conjugate is significantly different to that of the monomers. This too is likely to manifest itself as a local reduction in diffusion coefficient near the pattern edges. In fact, we do visibly see evidence of this reduction, as discussed below. It is also interesting to note that the calculations and experimental data for region 4 (shown in Figure 3c) do not agree with one another very well in contrast to the other two regions. We believe this is due to that region being the smallest, where confinement effects at high charge concentration (not accounted for in the model) will be amplified. With this region being very small, there will also be greater geometrical differences between the model and the actual experimental pattern, due to the limited resolution of our patterning technique.

As shown in Figure 2, there are two small rectangular patches of lipid bilayer beneath the main trap pattern. These were used as a reference for the analysis of the fluorescence intensity data. Interestingly, we found that the spatial intensity profiles in these, at any given time, were quite different as shown for example in the profile given in Figure 2d. Upon reversal of the applied field a mirror of this profile was observed, Figure 2e. To understand the origin of this behavior we undertook an experiment to map the spatial variation of the decay length (see Supporting Information) and have concluded that the electric field varies nonlinearly between the electrodes.

Size Effects in "Membrane Pumps". SU8 patterns of varying size were fabricated between interdigitated Au electrodes for testing the efficacy of diffusion-aided ratchets. The electrode spacing was varied between 292 and 632 μm providing much stronger electric fields for considerably lower applied potentials. The function of this pattern was to "pump" charged membrane components between two reservoirs, which could potentially be separated by an arbitrarily large distance. The device is operated by an ac electric field applied between the fingers. The double-sawtooth region connecting the two reservoirs served as a ratchet. On one-half of a cycle, the charges were driven into the gullets of one set of teeth. Then on the other half-cycle, the charges were driven into the gullets of the other set of teeth. The offset and asymmetry of the two sets of teeth caused a net motion toward the small reservoir with repeated cycling of the electric field. The time required to obtain a significant build-up was expected to be considerably less in these structures than the more macroscopic versions reported recently.[28]

Figure 4a shows the variable spaced interdigitated electrodes that were fabricated onto a 0.1 mm thick glass coverslip. The gaps between the electrode "fingers" were varied from 292 to 632 μm. The EggPC lipid bilayer containing 0.5 mol % negatively charged TR-DHPE lipid was formed between these fingers, using SU8 patterns as barriers. After rinsing with Milli-Q water, a 13 V ac sine wave potential with a period of 5 min was applied across the interdigitated electrodes. After 90 min, the relative concentration of TR-DHPE in each of the small reservoirs was determined, as described in the Experimental Section. The size of the structures sequentially reduced from row 1 to row 6 according to $[68(10 - n) + 20]$ μm where n is the row number (top to bottom, Figure 4 a). Since the same potential V was applied to each finger pair, the electric field strength E increased with row number according to $13V/[68(10 - n) + 20]$ μm. Figure 4b shows the experimental data (black squares) and simulated data (red circles) for the build-up as a function of patterns size (electric field). For smaller patterns, where the electric field was stronger, the accumulation of TR-DHPE in the rectangular reservoirs was larger, demonstrating a more efficient transfer of charged lipid by the ratchet pattern. For the smallest pattern with an electrode spacing of 292 μm, the relative concentration in the small reservoir reached around 2.8 after 90 min, while for the largest pattern with a dimension of 632 μm, the relative concentration was only 1.6. The trend shown by the fitted lines in Figure 4b indicates that the pump efficiency is higher for smaller patterns, where the electric field is correspondingly stronger. From the data shown in Figure 4b, it is evident that the build-up saturates at about 300 V/cm corresponding to an electrode separation of

dx.doi.org/10.1021/ac302446w | *Anal. Chem.* 2012, 84, 10702−10707

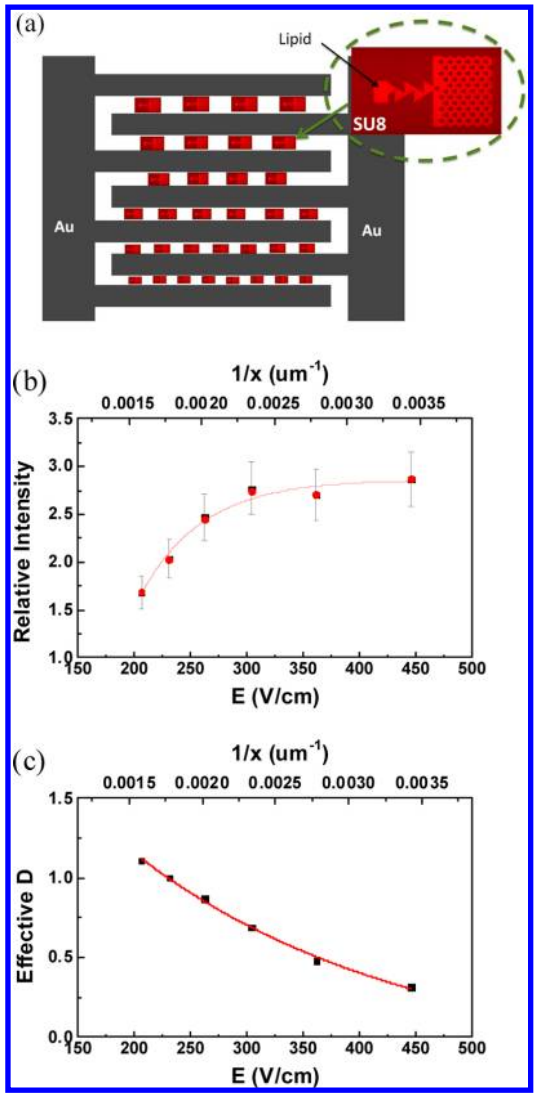

Figure 4. Transfer of TR-DHPE from a large reservoir to a smaller reservoir using asymmetrically patterned "pump" structures in SLBs. (a) Schematic showing the layout of the Au electrode (gray), SU8 patterns (dark red), and lipid bilayer (red) formed in the patterned structures. (b) The relative intensity in the small reservoirs after 90 min of applied ac sine wave potential, as a function of ac electric field amplitude. (c) The value of effective diffusion coefficient (D^*) used to give the best agreement between the experiment and the FEA calculation, as a function of ac electric field amplitude. x is the gap between the electrode fingers.

~430 μm. We note that the plateau in the relative intensity versus electric field is likely to arise as a consequence of self-quenching rather than the limit of maximum build-up being reached. Simulations performed for these patterns (and with the appropriate corresponding field strengths) required self-quenching and reduced diffusion coefficient to be included in order to accurately reflect the experimental data. In order to obtain the best agreement between simulation and experiment, the effective diffusion coefficient (D^*) was allowed to vary, as shown in Figure 4c. Interestingly, effective diffusion coefficient showed a monotonic decrease with increasing electric field strength, indicating that the effective diffusion coefficient of the TR-DHPE decreases in regions of high charged lipid concentration. Such a concentration dependent diffusion coefficient has been previously observed and is in agreement with other experiments performed by ourselves in which it was found that the diffusion coefficient of TR-DHPE in a POPC lipid bilayer decreased by more than 50% when the concentration of TR-DHPE was increased from 0.5 mol % to 2 mol %.[29−31] Such variation of effective diffusion coefficient with field strength is likely to be fluorophore specific and therefore requires further investigation to provide a more general understanding. Additionally, while we note that the potentials we are applying can lead to relatively large in-plane fields, these are small compared to those naturally found across native membranes. Further, AFM studies of bilayers before and after the application of electric fields have shown no evidence of bilayer deterioration.

Importantly we note that the operational time required to obtain the same level of build-up (i.e., to reach the self-quenching limit) is significantly reduced in the interdigitated electrode systems: from 16 to 1.5 h and with operation voltages reduced from 200 to 13 V.

CONCLUSIONS

The manipulation of charged lipids or proteins in supported lipid bilayers (SLBs) is important for many biological studies. By using asymmetrically patterned SLBs with applied ac electric fields, we have shown that it is possible to concentrate or directionally transport charged components in these systems. By reducing the electrode spacing, in addition to scaling down the lipid bilayer patterns, both the ac potential amplitude and experimental time required have been greatly reduced in comparison with our previous results. This ac electrophoretic method, which can operate at much lower voltages than dc electrophoresis, offers a versatile way to manipulate the charged components while they are maintained within a SLB. It is anticipated that future miniaturization of these devices may inspire the appearance of battery-driven portable lab-on-chip devices, for the sorting and concentration of charged membrane components, which would be particularly useful for membrane protein studies.

ASSOCIATED CONTENT

Supporting Information

Additional information as noted in text. This material is available free of charge via the Internet at http://pubs.acs.org.

AUTHOR INFORMATION

Corresponding Author

*Phone: +44(0)1133433852. E-mail: s.d.evans@leeds.ac.uk

Author Contributions

§P.B. and M.R.C. contributed equally to this work.

Notes

The authors declare no competing financial interest.

ACKNOWLEDGMENTS

The authors would like to acknowledge Wellcome Trust and the EPSRC for financial support on this project.

REFERENCES

(1) Yang, T. L.; Jung, S. Y.; Mao, H. B.; Cremer, P. S. *Anal. Chem.* **2001**, *73*, 165.
(2) Mao, H. B.; Yang, T. L.; Cremer, P. S. *Anal. Chem.* **2002**, *74*, 379.
(3) Gu, L. Q.; Braha, O.; Conlan, S.; Cheley, S.; Bayley, H. *Nature* **1999**, *398*, 686.
(4) Tamm, L. K.; McConnell, H. M. *Biophys. J.* **1985**, *47*, 105.

(5) Kam, L.; Boxer, S. G. *J. Am. Chem. Soc.* **2000**, *122*, 12901.
(6) Cremer, P. S.; Yang, T. L. *J. Am. Chem. Soc.* **1999**, *121*, 8130.
(7) Groves, T. J.; Mahai, L. K.; Bertozzi, C. R. *Langmuir* **2001**, *17*, 5129.
(8) Castellana, E. T.; Cremer, P. S. *Surf. Sci. Rep.* **2006**, *61*, 429.
(9) Spencelayh, M. J.; Cheng, Y. L.; Bushby, R. J.; Bugg, T. D. H.; Li, J. J.; Henderson, P. L. F.; O'Reilly, J.; Evans, S. D. *Angew. Chem.* **2006**, *45*, 2111.
(10) Sumino, A.; Dewa, T.; Kondo, M.; Mori, T.; Hashimoto, H.; Gardiner, A. T.; Cogdell, R. J.; Nango, M. *Langmuir* **2011**, *27*, 1092.
(11) Jonsson, P.; Gunnarsson, A.; Hook, F. *Anal. Chem.* **2011**, *83*, 604.
(12) Jonsson, P.; McColl, J.; Clarke, R. W.; Ostanin, V. P.; Jonsson, B.; Kleneman, D. *Proc. Natl. Acad. Sci. U.S.A.* **2012**, *109*, 10328.
(13) Engstler, M.; Pfohl, T.; Herminghaus, S.; Boshart, M.; Wiegertjes, G.; Heddergott, N.; Overath, P. *Cell* **2007**, *131*, 505.
(14) Gross, L. C. M.; Castell, O. K.; Wallace, M. I. *Nano Lett.* **2011**, *11*, 3324.
(15) Poo, M. M.; Robinson, K. R. *Nature* **1977**, *265*, 5595.
(16) Jaffe, L. F. *Nature* **1977**, *265*, 600.
(17) Daniel, S.; Diaz, A. J.; Martinez, K. M.; Bench, B. J.; Albertorio, F.; Cremer, P. S. *J. Am. Chem. Soc.* **2007**, *129*, 8072.
(18) Han, X.; Cheetham, M. R.; Sheikh, K.; Olmsted, P. D.; Bushby, R. J.; Evans, S. D. *Integr. Biol.* **2009**, *1*, 205.
(19) Stelzle, M.; Miehlich, R.; Sackmann, E. *Biophys. J.* **1992**, *63*, 1346.
(20) Groves, J. T.; Boxer, S. G. *Biophys. J.* **1995**, *69*, 1972.
(21) Groves, J. T.; Ulman, N.; Boxer, S. G. *Science* **1997**, *275*, 651.
(22) Groves, J. T.; Boxer, S. G.; McConnell, H. M. *Proc. Natl. Acad. Sci. U.S.A.* **1997**, *94*, 13390.
(23) Liu, C.; Monson, C. F.; Yang, T.; Pace, H.; Cremer, P. S. *Anal. Chem.* **2011**, *83*, 7876.
(24) Motegi, T.; Nabika, H.; Murakoshi, K. *Langmuir* **2011**, *28*, 6656.
(25) Oudenaarden, A. V.; Boxer, S. G. *Science* **1999**, *285*, 1046.
(26) Kashimura, Y.; Furukawa, K.; Torimitsu, K. *J. Am. Chem. Soc.* **2011**, *132*, 6118.
(27) Cheetham, M. R.; Bramble, J. P.; McMillan, D. G. G.; Krzeminski, L.; Han, X.; Johnson, B. R. G.; Bushby, R. J.; Olmsted, P. D.; Jeuken, L. J. C.; Marritt, S. J.; Butt, J. N.; Evans, S. D. *J. Am. Chem. Soc.* **2011**, *133*, 6521.
(28) Cheetham, M. R.; Bramble, J. P.; McMillan, D. G. G.; Bushby, R. J.; Olmsted, P. D.; Jeuken, L. J. C.; Evans, S. D. *Soft Matter* **2012**, *8*, 5459.
(29) Skaug, M. J.; Longo, M. L.; Faller, R. *J. Phys. Chem. B* **2011**, *115*, 8500.
(30) Saxton, M. J. *Biophys. J.* **1987**, *52*, 1046.
(31) Tsai, J.; Sun, E.; Gao, Y.; Hone, J. C.; Kam, L. C. *Nano Lett.* **2008**, *8*, 425.